

Research on Noise Suppression of Electronic Expansion Valve Aerated Super Cavitation Throttling

Rui Wang^{1, a}, Jing Liu¹, Yuhan Huang¹, Tao Yuan², Yueli Liu², Lifeng Wang², Zheng Du², Zeqi Li², Xiaojing You²

¹School of Civil Engineering, Henan Polytechnic University, Henan, China

²Institute of Building environment and Energy Efficiency, China Academy of Building Research, Beijing, China

^a1223982019@qq.com

Abstract

Due to the electronic expansion valve has the characteristics of wide adjustment range, high control precision, fast response and wide application range, it is widely used in the field of refrigeration and air conditioning and the throttling noise generated by the electronic expansion valve has also become a research hotspot. The researchers studied the structure, flow state and control scheme of the electronic expansion valve respectively. Based on the existing noise suppression methods, this paper proposes a new injection noise suppression method which is steam-filled super cavitation. The pressure distribution downstream of the orifice significantly inhibits cavitation and cavitation to achieves the purpose of reducing jet noise.

Keywords

Electronic expansion valve; Air entrainment super cavitation; Noise suppression.

1. INTRODUCTION

1.1. Throttle Valve Noise Generation Mechanism

Early research on throttling noise was mainly to clarify the mechanism of noise generation. Due to the gradual maturity of visualization tools and fluid simulation software, many scholars have carried out research on the structure, size and internal fluid flow state of electronic expansion valves, making the mechanism of throttling jet noise generation of electronic expansion valves more mature.

The flow noise of throttle valve has gradually attracted the attention of valve manufacturers and gradually entered the field of vision of scientific researchers since the middle of the 20th century. The International Electrotechnical Commission promulgated the valve noise prediction standard in 1955, which greatly promoted the study of noise. In 1985, Peizi Li et al established a theoretical basis for the valve noise generation mechanism through theoretical calculation and experimental research [1-2].

Russian scholars have carried out theoretical analysis and experimental research on the throttling noise of the regulating valve. Through the control of the parameters of the regulating valve in the experiment, the factors affecting the throttling noise of the regulating valve have been obtained [3]. Xiaosong Zhang et al of Southeast University judged the flow state of the refrigerant in the electronic expansion valve, and deeply studied the unique flow characteristics of the electronic expansion valve when the flow was blocked, which provided the conditions for realizing the optimal control of the electronic expansion valve and reducing the throttling noise

[4]. Xuewen Du et al. studied the noise characteristics of the throttle valve port. Based on the experiment, combined with the visual image and spectrum analysis, they revealed the basic law of the valve port cavitation noise, and proposed that the cavitation noise is the main factor of the throttle flow noise. [5]

Feng Chen, Jun Zhao and others analyzed the structure and flow rate of the electronic expansion valve. They found that the size and flow of the pilot hole have a great influence on the noise of the electronic expansion valve when the valve body flow rate increases, the valve body noise also increases. There is a certain positive correlation with it. [6]

1.2. Throttle Valve Noise Suppression Method

At present, the research mainly focuses on the factors that affect the throttling jet noise, such as the internal flow channel structure of the throttling device, the characteristics of the fluid medium, the size and the inlet and outlet pressures. Russian scholars carried out theoretical calculations and experiments on the regulating valve, effectively analyzed the experimental results, and designed a new model with relatively smooth streamlines, which effectively reduced the noise and increased the flow rate [3]. Through the experimental research on the fluid noise of the throttle valve, Xuewen Du and others from Zhejiang University of Technology designed a new valve port structure using the principle of two-stage throttling and partial pressure, which reduced cavitation and largely suppressed the generation of cavitation noise [5].

Fang Liang et al. conducted experimental research on the traditional throttle valve and the side-hole electronic expansion valve with the poppet valve as the flow port, and analyzed the flow characteristics, valve opening and leakage performance, and analyzed the performance of flow control and noise. Inhibition provides a theoretical basis. Du Yi [7] analyzed the noise at the outlet of the electronic expansion valve from the perspective of aeroacoustics. Through numerical simulation and experiments, he designed a two-stage throttling device with a capillary tube and an electronic expansion valve, which achieved the effect of suppressing noise, but the structure was complex.

Based on the original jet noise suppression method, this paper proposes a new noise suppression method super cavitation with steam.

2. MATHEMATICAL MODEL OF FLUID FLOW IN ELECTRONIC EXPANSION VALVE

Due to the fluid in the electronic expansion valve changes drastically before and after throttling, Fluent is very convenient and adaptable to solve various fluid problems. Therefore, we will use Fluent to numerically simulate the fluid flow in the electronic expansion valve. The physical and mathematical models used in the calculation and simulation will be introduced below.

2.1. Conservation Equations in Mixed Multiphase Flow Models

The conservation equation of the model is:

$$\frac{\partial}{\partial t}(\rho) + \nabla \cdot (\rho \vec{V}) = 0 \quad (1)$$

In the formula: the parameter ρ is the density, \vec{V} is the quantized speed.

Momentum conservation equation:

$$\frac{\partial}{\partial t}(\rho_m v_m) + \nabla \cdot (\rho_m v_m^2) = -\nabla p + \nabla \cdot [\mu_m(\nabla v_m + \nabla v_m^T)] + \rho_m g + F + \nabla \cdot \left(\sum_{k=1}^n \alpha_k \rho_k v_{dr,k}^2 \right) \quad (2)$$

where p represents the hydrostatic pressure, μ_m represents the dynamic viscosity of the mixture, F represents the source term, α_k represents the size ratio of the k th term, ρ_k represents the density of the k th phase, $v_{dr,k}$ represents the drift velocity of the k th phase.

Energy conservation equation:

$$\frac{\partial}{\partial t} \sum_{k=1}^n (\alpha_k \rho_k E_k) + \nabla \cdot \sum_{k=1}^n [\alpha_k v_k (\rho_k E_k + p)] = \nabla \cdot (k_{eff} \nabla T) + S_E \quad (3)$$

$$E_k = h_k - \frac{P}{\rho_k} + \frac{v_k^2}{2} \quad (4)$$

In this formula E_k represents the energy of the k th phase, v_k represents the velocity of the k th phase, k_{eff} represents the ability to transfer internal energy, S_E represents the energy exchange phase.

In this paper, HFC-410A refrigerant is selected as the fluid in the electronic expansion valve for research. The gaseous HFC-410A volume fraction equation:

$$\frac{\partial}{\partial t}(\alpha_k \rho_k) + \nabla \cdot (\alpha_k \rho_k v_m) = -\nabla \cdot (\alpha_k \rho_g v_{dr,1}) + (m_{1g} + m_{g1}) \quad (5)$$

In this formula the subscript g represents the gas phase and m_{1g} & m_{g1} represents the mass exchange phase.

The momentum equation in the hybrid model only calculates the average value of the velocity, and the momentum source term caused by the mass exchange during the phase transition is not considered. After optimization, it is only necessary to supplement the mass exchange terms m_{1g} & m_{g1} and energy exchange terms of equations (3) and (5) to obtain the equation to be solved. All the above equations are determined according to the refrigerant flash phase transition model [8].

When the refrigerant flows in the pipeline, the approximate boiling process that occurs when the temperature of the fluid is higher than the saturation temperature corresponding to the local pressure is called the flashing process. The mass transfer between the two phases and the energy source of the gas-phase refrigerant in the energy equation can be calculated according to equations (6) and (7).

$$m_{1g} = \frac{-\gamma \rho_1 \alpha_1 (T_1 - T_{sat}^p)}{T_{sat}^p} \quad (6)$$

$$S_E = m_{1g} \cdot h_{sat}^T \quad (7)$$

T_{sat}^p represents the boiling point of the refrigerant when the pressure is p , γ is the relaxation factor of the time term, used in the iterative calculation, and is used to obtain the mass transfer rate in the grid, and its size is also closely related to the time step of the

instantaneous calculation [9]. The experimental data in table 1 can be used to derive the above-mentioned expressions.

Table 1. Corresponding reference values under the saturated state of Freon

Pressure /Mpa	Temperature /K	Standard enthalpy /(kj/kg)
0.4	253.1	287.90
0.6	264.4	282.22
0.8	272.9	278.30
1.0	280.3	274.70
1.5	294.5	267.47
2.0	305.4	261.70
2.5	314.4	256.82
3.0	322.1	252.55
3.5	328.9	248.70

2.2. Fluid Turbulence Model

In this paper the turbulence model used in the numerical simulation is a realizable turbulence model. This model has high calculation accuracy and good stability, it can calculate most fluid flow problems from low Reynolds number to high Reynolds number, especially for jet and wake. Special flow problems such as flow, swirling flow etc. The following is an introduction from the turbulence model, turbulent viscosity and wall function.

2.2.1. Achievable $\kappa - \epsilon$ Turbulence Model

Realizable model where X and Y can be obtained from the following two equations.

$$\frac{\partial}{\partial t}(pk) + \frac{\partial}{\partial x_j}(\rho k u_j) = \frac{\partial}{\partial x_j} \left[\left(\mu + \frac{\mu_t}{\sigma_k} \right) \frac{\partial k}{\partial x_j} \right] + G_k + G_b - \rho \epsilon - Y_M + S_k \tag{8}$$

$$\frac{\partial}{\partial t}(\rho \epsilon) + \frac{\partial}{\partial x_j}(\rho \epsilon u_j) = \frac{\partial}{\partial x_j} \left[\left(\mu + \frac{\mu_t}{\sigma_\epsilon} \right) \frac{\partial \epsilon}{\partial x_j} \right] + \rho C_{1\epsilon} S_\epsilon - \rho C_{2\epsilon} \frac{\epsilon^2}{k + \sqrt{\nu \epsilon}} + C_{1\epsilon} \frac{\epsilon}{k} C_{3\epsilon} G_b + S_\epsilon \tag{9}$$

Where $C_{1\epsilon} = \max \left[0.43, \frac{\eta}{(\eta+5)} \right]$, $\eta = \frac{S K}{\epsilon}$, $S = \sqrt{2 S_{ij} S_{ij}}$, $C_{1\epsilon}$ and $C_{2\epsilon}$ are constants.

$$G_k = -\rho \left(\frac{\partial u_i}{\partial x_j} + \frac{\partial u_j}{\partial x_i} \right) \frac{\partial u_i}{\partial x_j} \tag{10}$$

For incompressible fluids, there is $G_b = 0$. For compressible fluids

$$G_b = \beta g_i \frac{\mu_i}{pr_t} \frac{\partial T}{\partial x_i} \tag{11}$$

The Prandtl number pr_t is usually set to 0.85 and the expansion coefficient can be obtained from the following formula

$$\beta = -\frac{1}{\rho} \frac{\partial \rho}{\partial T} \quad (12)$$

When the fluid is incompressible, the overall dissipation rate is affected by gap expansion $Y_m = 0$. When the fluid is compressible

$$Y_M = 2\rho\varepsilon M_t^2 \quad (13)$$

2.2.2. Turbulent viscosity equation

Generally, the following relationship is used to calculate the fluid viscosity parameters

$$d\left(\frac{\rho^2}{\sqrt{\varepsilon\mu}}\right) = 1.72 \frac{\hat{v}}{\sqrt{\hat{v}^3 - 1 + C}} d\hat{v} \quad (14)$$

Under the condition of high Reynolds number, the turbulent viscosity coefficient μ_t is calculated as

$$\mu_t = \rho C_\mu \frac{k^2}{\varepsilon} \quad (15)$$

$C_\mu = \frac{1}{(A_0 + A_s \frac{kU}{\varepsilon})}$ is a function of the angular velocity, the mean stress value and the rotation

rate in the rotating system. $U = \sqrt{S_{ij}S_{ij} + \vec{\Omega}_{ij}\vec{\Omega}_{ij}}$, $\vec{\Omega}_{ij} = \Omega_{ij} - 2\varepsilon_{ijk}\omega_k$, $\Omega_{ij} = \vec{\Omega}_{ij} - \varepsilon_{ijk}\omega_k$, $\vec{\Omega}_{ij}$ represent the average rotation rate of the angular velocity in the movable reference frame. Except $A_0 = 4.04$, $A_s = \sqrt{6} \cos \theta$, $\theta = \frac{1}{3} \cos^{-1}(\sqrt{6}W)$, $W = \frac{S_{ij}S_{jk}S_{ki}}{S^3}$, $\vec{S} = \sqrt{S_{ij}S_{ij}}$, $S_{ij} = \frac{1}{2} \left(\frac{\partial u_j}{\partial x_i} + \frac{\partial u_i}{\partial x_j} \right)$.

2.2.3. Wall function

The internal flow of the electronic expansion valve belongs to the high Reynolds number flow, and the speed difference in the vertical direction of the speed is very large in the place close to the pipe wall. In order to better select the calculation method of the flow field in this area, it is necessary to use the parameters y^+ . The dimensionless wall distance is expressed as:

$$y^+ = \frac{y\rho\mu_\tau}{\mu} \quad (16)$$

Due to the high flow Reynolds number, this paper chooses the wall function to solve the boundary layer flow. The wall function requires the mesh size of the first layer to satisfy $30 < y^+ < 300$, and uses the parameter y^+ to solve for the height $y = \frac{y^+\mu}{(U_\tau\rho)}$ of the first layer mesh. There are many kinds of wall function processing methods. Based on the non-equilibrium wall function method, it can accurately analyze the wall pressure gradient and more accurately calculate the characteristics of the turbulent kinetic energy corresponding to the wall mesh. The next numerical simulation chooses the non-equilibrium wall function method.

3. NUMERICAL SIMULATION OF ELECTRONIC EXPANSION VALVE

3.1. Electronic Expansion Valve Model

This article takes a certain type of electronic expansion valve provided by domestic air-conditioning accessories manufacturers as an example. The specific model is shown in Figure 1. The electronic expansion valve adjusts the current pulse to control the rise and fall of the valve needle in the valve body to adjust the opening of the electronic expansion valve to achieve the effect of controlling the refrigerant flow and evaporation temperature.

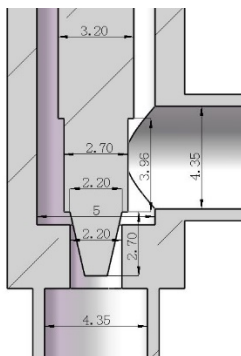


Figure 1. Dimensions of electronic expansion valve (mm)

Since the pulse amplitude of the electronic expansion valve is 0-500 pulses, and generally used between 100-400 pulses, this paper selects 100, 200, 300, and 400 pulses for simulation. Because the number of pulses of the motor is proportional to the rising height of the valve needle, and the number of pulses is not enough to describe the pulse opening. Therefore, we convert the number of pulses we use into the rising height of the valve needle. When the pulse is 0, the position of the valve needle is the reference plane. The relationship is shown in Table 2 below:

Table 2. Pulse and valve needle lift height

number of pulses	Valve needle rise height/(mm)	number of pulses	Valve needle rise height / (mm)
100	0.54	300	1.62
200	1.08	400	2.16

The flow field model diagrams of the four openings are shown in Figures 2 and 3 below:

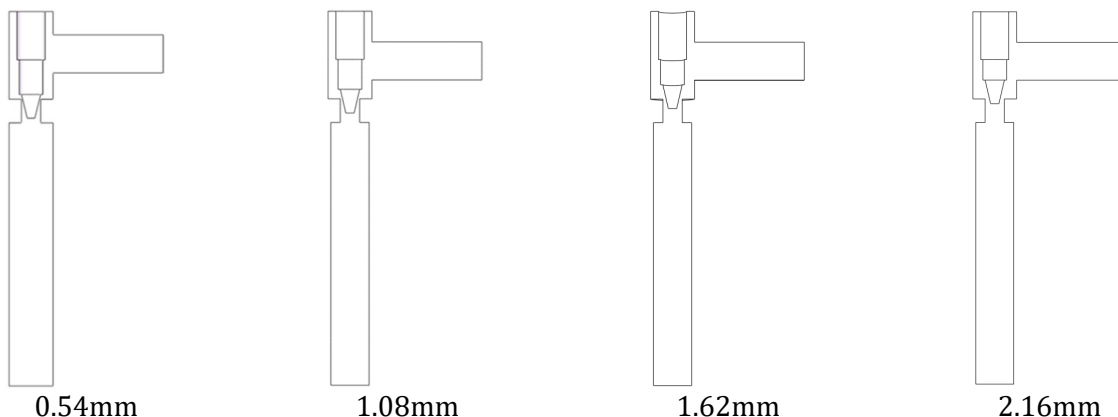


Figure 2. Flow field diagram of the original model

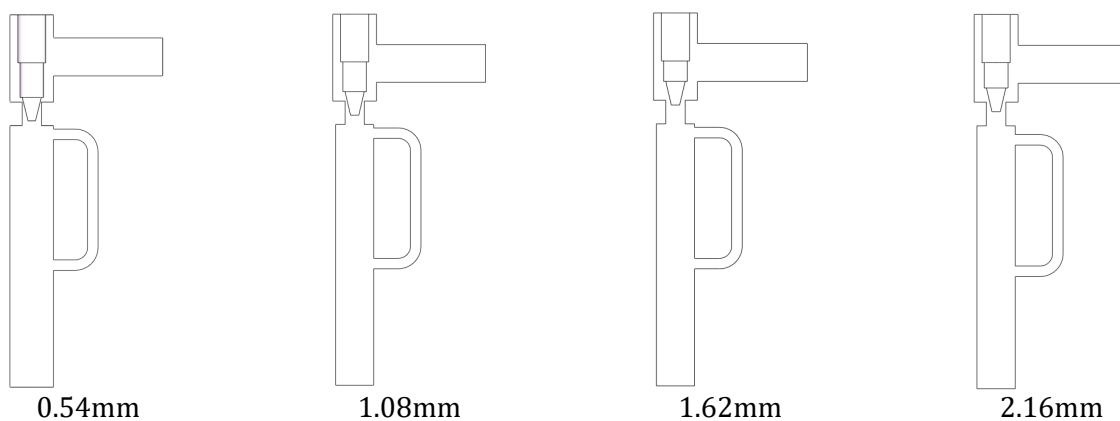


Figure 3. Flow field diagram of the improved model

3.2. Meshing and Independence Analysis

Since the flow channels of the inlet and outlet sections are relatively regular, the structural hexahedral mesh is used for division, which can not only improve the calculation accuracy, but also reduce the mesh size and speed up the calculation progress. For the valve needle and the complex flow channel around it, this paper uses unstructured tetrahedral mesh to divide it, and at the same time, the junction of the wall is refined to ensure that the mesh quality can meet the calculation requirements. In the following, the runner model with 1.62mm opening is divided into different densities of meshes, and the number of meshes is 392,000, 933,000, and 1.281 million. In order to ensure the accuracy of the calculation, the meshes at the connection and the valve needle are respectively After encryption, the result is shown in Figure 4 below. The above meshing is completed in Ansys mesh.

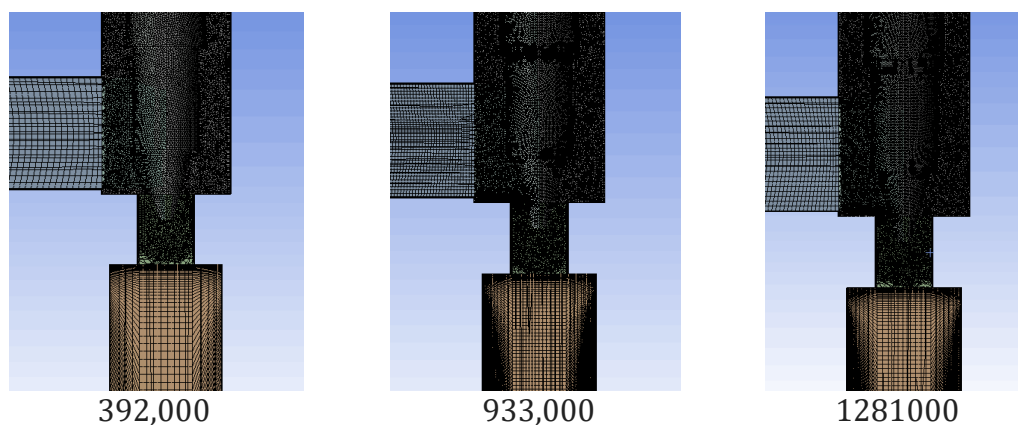


Figure 4. Grid comparison under different sizes

The simulation results obtained by fluent are as follows:

Table 3. Flow and speed of inlet and outlet of electronic expansion valve

number of grids	Ingress traffic (g/s)	Egress traffic (g/s)	Maximum speed (m/s)	Throat gas volume (%)
312000	104.9	105.6	65.64	26.5
933000	107.8	107.4	69.01	24.8
1281000	108.6	108.5	71.24	22.8

Through the comparison of the above data, it is found that the simulation results of the three grids are not very different, especially the simulation results of 933,000 and 1.281 million are very close, and the difference of each parameter is within 1%. Therefore, it can be proved that the simulation is carried out with the number of 933,000 meshes, and the result is very small.

3.3. Turbulence Functions and Boundary Conditions

The turbulent viscosity calculation formula and momentum equation in the model are more refined, which can meet the constraints of eddy current disturbance calculation and Reynold's stress and can ensure that the simulation results are as close to the actual situation as possible, and more accurate results can be obtained. Therefore, the model is selected in this paper. At the same time, since non-Equilibrium is suitable for most Reynolds number situations, it does not require high mesh quality in the near-wall area and has high calculation accuracy, so the wall function uses an unbalanced wall function.

The inlet and outlet pressure of the electronic expansion valve can be measured through experiments, so the pressure inlet and outlet are set; considering the actual situation, the fluid at the inlet of the electronic expansion valve has a certain degree of subcooling, so the dryness of the inlet is set to 0; When flowing through the valve body, the flow velocity is very fast, which will form a low pressure in the local area of the valve body, which will cause cavitation. This paper selects the cavitation model. The pressure conditions of the inlet and outlet of the electronic expansion valve under different opening degrees measured by the experiment are shown in Tables 4 and 5.

Table 4. The corresponding inlet and outlet conditions of the electronic expansion valve under different opening degrees under the rated working conditions before the improvement

Opening (mm)	0.54	1.08	1.62	2.16
inlet pressure (Mpa)	1.5	2.75	3.2	3.7
Outlet pressure (Mpa)	0.71	0.8	0.95	1.2
inlet temperature (°C)	6.5	14.2	13.6	24
Outlet temperature (°C)	13	14.5	15	21.5

Table 5. The corresponding inlet and outlet conditions of the electronic expansion valve under different opening degrees under the improved rated operating conditions

Opening (mm)	0.54	1.08	1.62	2.16
inlet pressure (Mpa)	1.49	2.74	3.17	3.68
Outlet pressure (Mpa)	0.70	0.79	0.92	1.18
inlet temperature (°C)	6.4	14.1	13.5	23.8
Outlet temperature (°C)	12.9	14.3	14.9	21.3

3.4. Laboratory Equipment and Procedures

A refrigerator is used to conduct experimental research on the noise of the electronic expansion valve, and the following experimental equipment is used:

(1) Prefabrication of refrigerators

A normal working air-cooled inverter refrigerator.

Accessories and parts

Loose parts must be fixed

(2) Noise measurement equipment

- Germany Siemens noise measurement equipment
- Noise collection microphone
- Acquisition signal amplifier
- (3) Air-entrained noise reduction device

Table 6. Refrigerator noise experimental instruments and models

No.	Name	Model	Remarks
1	refrigerator	BCD-520WICTU1	D×W×H = 677×830×1908 mm
2	Noise measurement equipment	SIEMENS	
3	Noise Picking Microphone	UC-59	
4	Acquisition signal amplifier	NH-22A	

The specific experimental steps are as follows:

(1) Experimental conditions

The experiment was carried out in a semi-anechoic chamber, and the ambient temperature was kept within the range of $25\pm 0.5^{\circ}\text{C}$; the relative humidity of the environment was maintained within the range of $(55\pm 1)\%$; the indoor air velocity was lower than 0.25m/s.

(2) Experimental steps

Place the refrigerator in the geometric center of the semi-anechoic chamber, check and close the door after placing it smoothly.

Let the refrigerator run under no-load state, set the temperature controller to keep the fresh-keeping room at 5°C , and run the test for at least 30 minutes before starting the test. If the compressor stops during the test, you need to interrupt the measurement and wait for the compressor to restart for 3 minutes to start again.

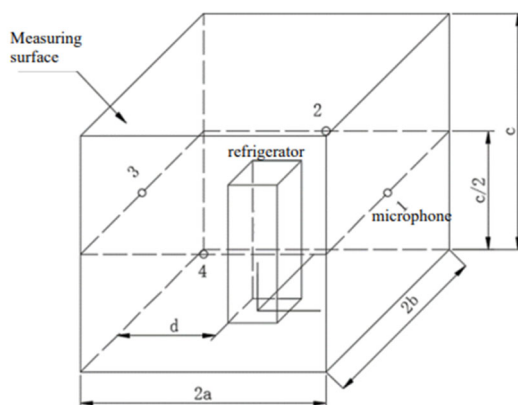


Figure 5. Schematic diagram of noise measurement layout

According to the rectangular envelope method in the national standard GB-T8059, arrange the measuring points around the refrigerator, a total of 4 points, as shown in Figure 5, adjust the height and distance, and preheat the equipment.

Start the measurement after the refrigerator runs stably for 3 cycles.

Renovate the outlet of the electronic expansion valve of the refrigerator, install an aeration device, and repeat the above steps to carry out the experiment.

Analyze the experimental data before and after improvement and draw conclusions.

4. RESULT ANALYSIS

In this simulation, by monitoring the difference between the inlet and outlet flow of the electronic expansion valve, when the difference between the inlet and outlet flow is within the allowable error range and does not change with the calculation time step, the calculation can be considered to have converged. By comparing the mass flow measured in the experiment and the mass flow in the simulation calculation, it is found that the flow values under different openings are very close. It can be considered that the numerical simulation meets the requirements, and the mass flow curve is shown in the following table.

Table 7. Comparison of inlet and outlet flow of electronic expansion valve

	Import mass flow kg/s	outlet mass flow kg/s	Relative error %
Original Electronic Expansion Valve	0.04574	0.04425	3.26
add bypass	0.04417	0.04281	3.08

4.1. Velocity Vector Analysis

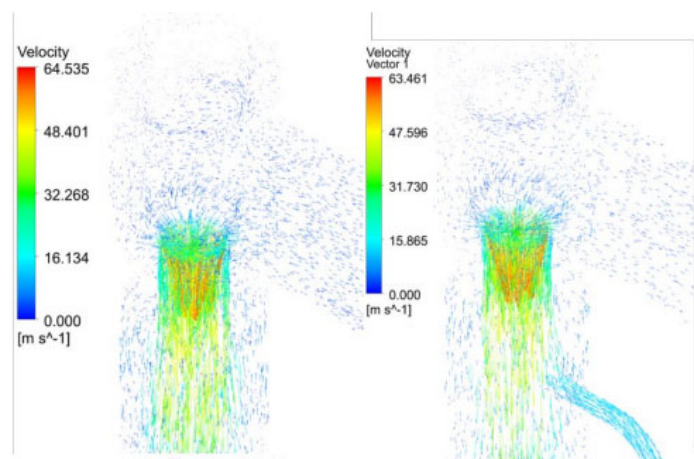


Figure 6. Vector diagram of the throat velocity distribution of the electronic expansion valve before and after the improvement of the 0.54mm opening

As shown in Figure 6, the flow of refrigerant is relatively intense at the outlet of the electronic expansion valve, and the flow rate of the refrigerant at the needle valve and the outlet reaches the highest. reduced to 63.46 m/s. According to the cavitation dynamics and Light hill noise theory, the outlet velocity of the electronic expansion valve decreases and the local pressure increases, which can effectively prevent the refrigerant bubbles at the outlet of the electronic expansion valve from bursting, and the noise generated by the jet is reduced. The flow rate of the agent is significantly reduced.

4.2. Turbulent Kinetic Energy Distribution

Noise is closely related to fluid turbulent kinetic energy. As shown in Figure 13, from the overall observation, observing the turbulent kinetic energy of the aeration position at the outlet of the electronic expansion valve, it is found that the turbulent kinetic energy at the outlet of the electronic expansion valve is significantly reduced. The turbulent kinetic energy at the comparison position line is shown in Figure 14, which shows that after applying the aeration

device, the turbulent kinetic energy at the aeration position can be effectively reduced by 12.5%-86.7%, which can effectively reduce the turbulent kinetic energy at the outlet of the electronic expansion valve and reduce noise.

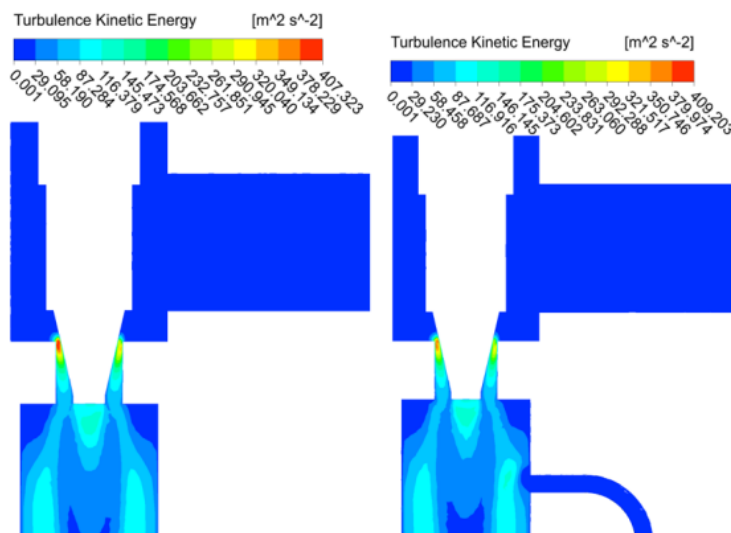


Figure 7. Cloud diagram of turbulent kinetic energy distribution in the throat of electronic expansion valve before and after improvement of 0.54mm opening

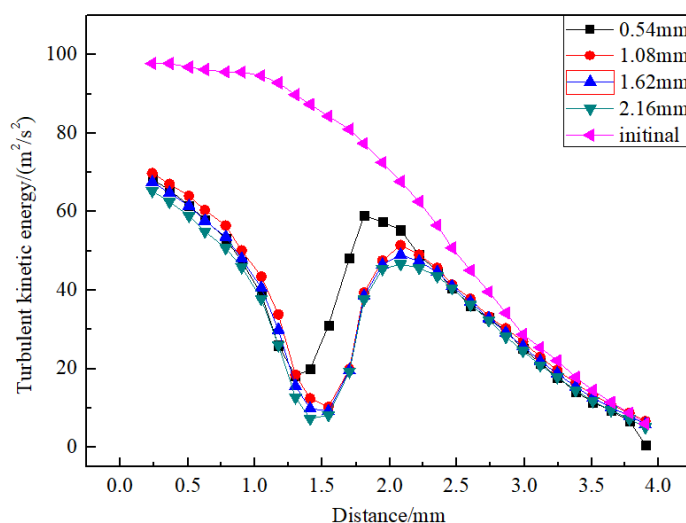


Figure 8. Turbulent kinetic energy distribution of electronic expansion valve throat before and after improvement with different opening degrees

4.3. Gas phase Volume Distribution

As shown in Figure 9, comparing the volume fraction of the local gas phase with aeration at the outlet of the electronic expansion valve and that without aeration, the volume fraction of the local gas phase after aeration is significantly higher than that before the aeration and is affected by the opening of the electronic expansion valve. Smaller, as shown in Figure 10, compared with the gas phase volume fraction at each position line increased by 0.81% - 0.93%, indicating that after aeration, the refrigerant in the evaporator inlet pipe was introduced into the outlet of the electronic expansion valve, increasing the local pressure, the electronic expansion valve. The growth, maturation and collapse of bubbles at the outlet are inhibited.

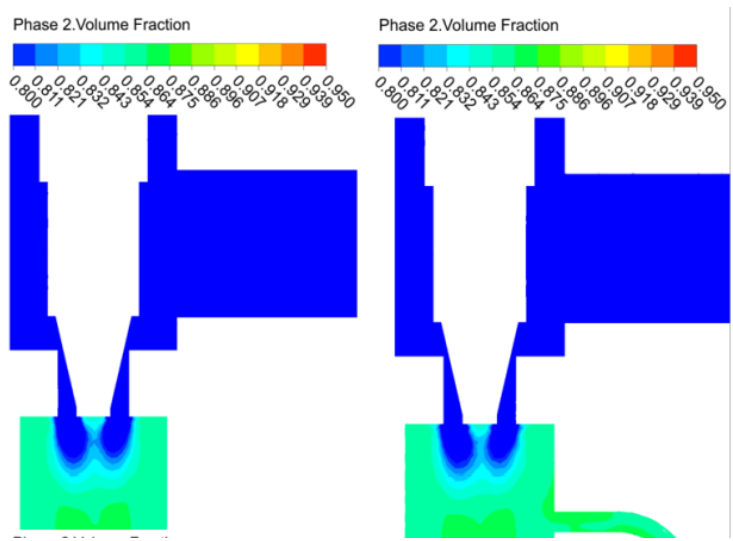


Figure 9. Cloud map of gas phase volume fraction distribution in the throat of electronic expansion valve before and after the improvement of 0.54mm opening

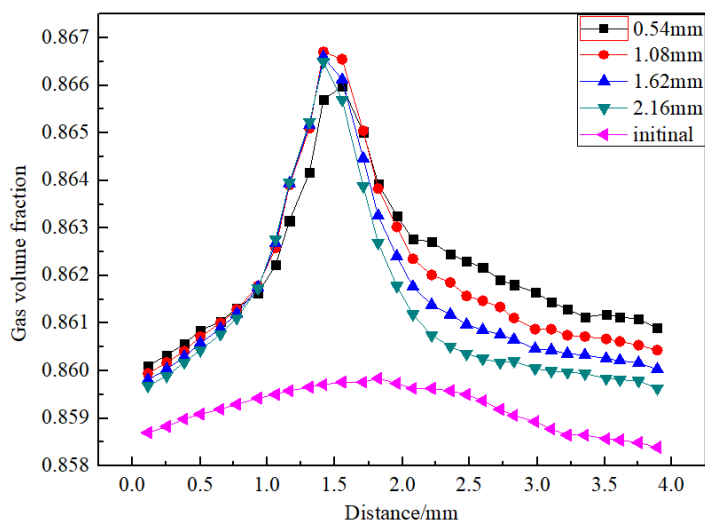


Figure 10. Volume fraction distribution of gas phase in the throat of electronic expansion valve before and after improvement with different opening degrees

4.4. Noise Sound Power

Further detailed analysis of the sound power flowing at the outlet of the electronic expansion valve, as shown in Figure 11, it can be found that after the bypass pipe is installed for aeration, the sound power has been greatly reduced at the aeration position. Analysis of the sound power at the aerated position is shown in Figure 12. Compared with the position without the bypass pipe, the rising power can be reduced by 3.0dB-9.5dB. When the opening is 2.16mm, the effect is the best, and when the opening is 0.54mm, it is the worst effect.

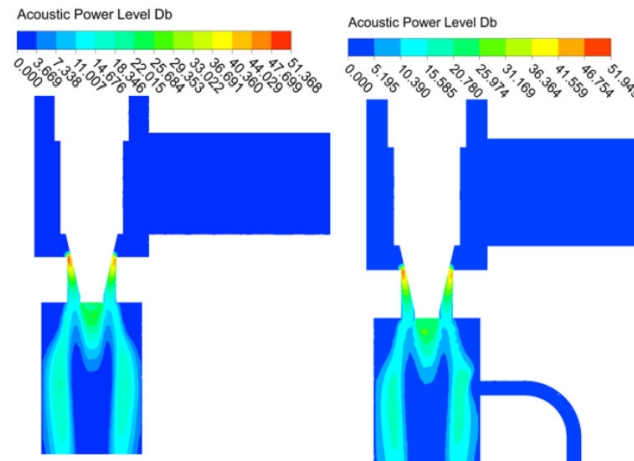


Figure 11. Cloud map of sound power distribution in the throat of the electronic expansion valve before and after the improvement of the 0.54mm opening

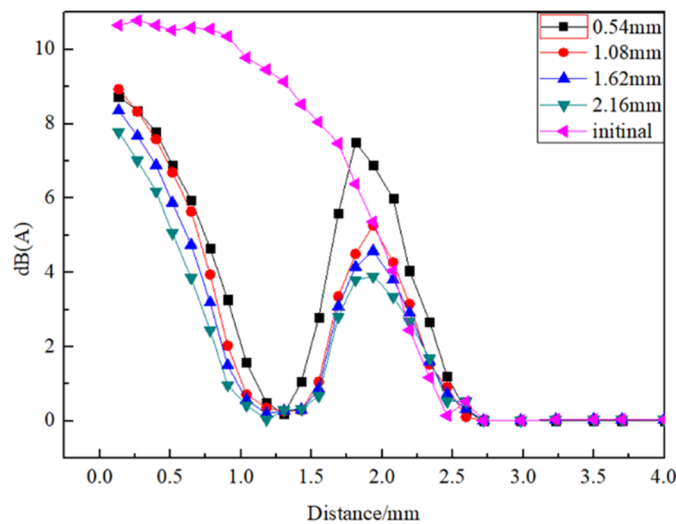


Figure 12. Sound power distribution of electronic expansion valve throat before and after different improvements

4.5. Analysis of Results

The simulation results are verified by experiments, and the following experimental data are obtained, as shown in Figure 13.

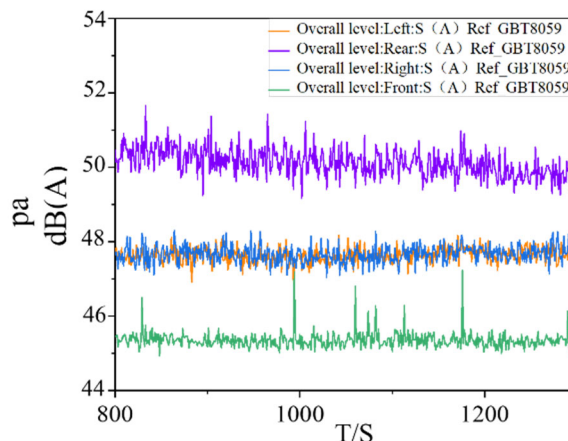


Figure 13. Sound power distribution of electronic expansion valve throat before improvement with different openings

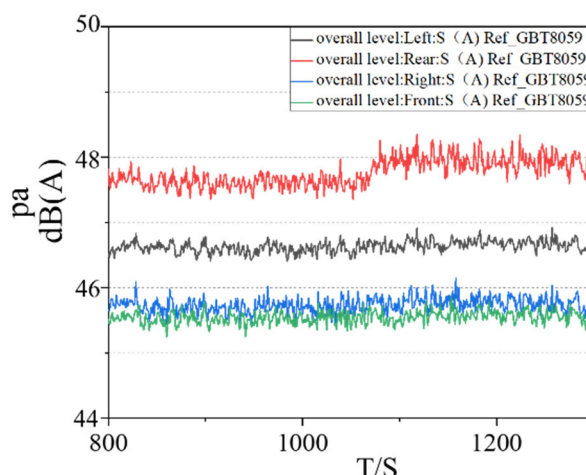


Figure 14. Sound power distribution of electronic expansion valve throat after different openings are improved

(1) The noise values on the right and rear are too large, because the microphones on the right and rear are closer to the outlet of the electronic expansion valve in the refrigerator compartment, so the measured noise values will be higher than the other two.

(2) By installing an aeration device at the outlet of the electronic expansion valve of the refrigerator and using the bypass pipe to reintroduce the evaporated refrigerant gas to the outlet of the electronic expansion valve, the low-pressure area generated at the outlet of the electronic expansion valve can be offset, and the electronic expansion valve can be significantly improved. The local pressure at the valve outlet can suppress the collapse of the refrigerant bubbles, thereby suppressing the bubble burst noise. By comparing the time domain Figure 13 and Figure 14, it can be found that after the aeration device is installed at the outlet of the electronic expansion valve, the overall noise of the refrigerator decreased by 2.5dB(A).

5. CONCLUSION

Using the theory of aeration super cavitation, the structure of the electronic expansion valve is optimized, and the noise suppression research is carried out.

1) From the overall point of view, the influence of the aeration device on the inlet and outlet temperature and pressure of the electronic expansion valve is less than 0.5%; from a local point of view, after aeration, the local pressure is effectively increased by 0.005-0.015Mpa, which can effectively inhibit the electronic expansion valve. The growth, maturity and collapse process of bubbles at the outlet reduce the noise caused by bubble bursting.

2) Comparing the turbulent kinetic energy at the outlet of the electronic expansion valve, it is found that the turbulent kinetic energy is reduced by 15.5%-19.6%, which can effectively reduce the turbulent kinetic energy at the outlet of the electronic expansion valve and reduce the noise.

3) After aeration, the local gas phase volume fraction is significantly increased compared with that before the aeration, and the gas phase volume fraction is increased by 0.81%-0.93%, indicating that after aeration, the intensity of cavitation is effectively reduced. The outlet of the electronic expansion valve The growth, maturation and collapse of bubbles are inhibited.

4) Comparative analysis of the gas phase distribution diagram and sound power diagram with or without aeration device at the outlet of the electronic expansion valve, it is found that the aeration device can effectively increase the local pressure of the throat, inhibit the bursting of refrigerant bubbles, and inhibit cavitation. Reduce the noise generation, reduce the noise by 3.0dB-9.5dB, when the opening is 2.16mm, the effect is the best.

REFERENCES

- [1] Genhua Dai, Hongyu Wang, Peizi Li: Low noise valve design principle and valve noise control. *Noise and Vibration Control*, Vol.05 (1985) No. 5, p.22-24+28.
- [2] Peizi Li, Xiaoyang Huang: The control effect of small orifice plate on valve noise and its influence on valve flow control. *Acta Scientiae Circumstantiae*, Vol. 6 (1986) No. 3, p. 343-352.
- [3] Shan Tu, Jingru Mao, Bi Su: A review of research on control valve instability induced by unsteady complex flow. *Fluid Machinery*, Vol. 28 (2000) No. 4, p. 30-32.
- [4] Caihu Liang, Xiaosong Zhang, Shuxiong Li: Research on blocking flow effect on control of electronic expansion valve. *Journal of Southeast University (Natural Science Edition)*, Vol. 35 (2005) No. 1, p. 77-81
- [5] Xuewen Du, Xin Fu: Noise characteristic and control method of throttling valve. *Fluid Power Transmission and Control*, Vol. 7 (2009) No. 6, p. 27-29
- [6] Feng Chen, Jun Zhao: Analysis and Discussion on the relationship between the noise of electronic expansion valve and guide sleeve for air condition, *China Plant Engineer*, Vol. 35 (2019) No. 01, p. 103-104
- [7] Yi Du. Research on aero dynamic noise and noise reduction of air-conditioner electronic expansion valve. *Journal of China University of Metrology (MS, China Jiliang University, Chian, 2018)*, P. 64
- [8] Yongguang Nie, Yu Mao, Jiangyun Wang, Jun Wang: Research on aero dynamic noise and noise reduction of air-conditioner electronic expansion valve. *Acta Petrolei Sinica (Petroleum Processing Section)*, Vol. 28 (2012) No. 5, p. 814-820.
- [9] S. Prasanth Kumar, B.V.S.S.S. Prasad, G. Venkatarathnam, K. Ramamurthi, S. Srinivasa Murthy. Influence of surface evaporation on stratification in liquid hydrogen tanks of different aspect ratios. *International Journal of Hydrogen Energy*, Vol. 32 (2007) No. 12, p. 1954-1960.